Journal of Alloys and Compounds 500 (2010) 78–81

Contents lists available at ScienceDirect

Journal of Alloys and Compounds

journal homepage: www.elsevier.com/locate/jallcom

Preparation and characterization of $CuInSe_2$ thin films by chemical bath deposition technique

P.P. Hankare[a,*], K.C. Rathod[a], P.A. Chate[a], A.V. Jadhav[a], I.S. Mulla[b]

[a] Department of Chemistry, Shivaji University, Kolhapur, MH 416004, India
[b] National Chemical Laboratory, Pune 411008, India

ARTICLE INFO

Article history:
Received 19 November 2009
Received in revised form 19 March 2010
Accepted 25 March 2010
Available online 2 April 2010

Keywords:
Thin films
Optical properties
X-ray diffraction
$CuInSe_2$

ABSTRACT

Copper indium diselenide (CIS) thin films have been deposited using a precursor solution containing copper sulphate, indium trichoride, hydrazine hydrate and sodium selenosulphate in an aqueous alkaline medium at room temperature. The as grown brown colored films were found to be well adherent to glass substrates. The films were characterized by X-ray diffraction, scanning electron microscopy, atomic absorption spectroscopy, optical absorption, electrical resistivity, and thermo electric measurement techniques. The analysis of optical absorption data shows band-gap energy (E_g) to be 1.1 eV. The electrical resistivity of the thin film was found to be of the order of 10^2 (Ω cm). Thermoelectric power measurement shows n-type conduction.

1. Introduction

For the sake of environmental protection and energy conservation, a cheap and clean source of renewable energy is essential for mankind [1]. Copper indium diselenide ($CuInSe_2$) has been one of the most promising photovoltaic materials because of its optical and electrical properties [2,3]. In the form of thin film, it is most promising due to its low energy band-gap (1.1 eV) and high absorption coefficient; their solar cells have been reported to have ~18% efficiency [4–7]. It can be deposited by various techniques such as, molecular beam epitaxy (MBE) [8], chemical vapour deposition (CVD) [9], evaporation [10], RF sputtering [11] and electrodeposition [12,13] etc.

In the present investigation, we have successfully synthesized $CuInSe_2$ (CIS) thin film on non-conducting glass slides by chemical bath deposition technique (CBD) from aqueous alkaline medium. The preparation parameters such as pH, deposition time and deposition temperature have been studied so as to obtain good quality $CuInSe_2$ films. The structural and morphological characterizations of films have been carried out by X-ray diffraction (XRD), scanning electron microscopy (SEM), and their optical and electrical properties have been studied by UV–VIS–NIR spectrophotometer and thermoelectric measurements.

2. Experimental

2.1. Substrate cleaning

The substrates were cleaned by boiling them in chromic acid for 1 h, followed by washing successively with detergent solution and alcohol. Substrates were finally stored under double distilled water before use.

2.2. Reagents and preparation of solutions

All the chemicals used for the preparation of CIS thin films were of AR grade. The solutions were prepared in double distilled water. Sodium selenosulphate (0.2 M) was prepared by refluxing 5 g of selenium powder with 15 g of sodium sulphite in 200 mL of double distilled water for 9 h at 363 K [14].

2.3. Synthesis of $CuInSe_2$ thin films

The deposition of CIS thin film was made from a reactive solution obtained by mixing 5 mL (0.2 M) copper sulphate, 5 mL (0.2 M) indium trichloride, 2.5 mL (1 M) tartaric acid, 10 mL (2%) hydrazine hydrate and 10 mL (0.2 M) sodium selenosulphate and finally diluted to 80 mL by adding double distilled water. The beaker containing the reactive solution was kept at the room temperature (300 K). The pH of the resulting solution was found to be 10 ± 0.05. Four cleaned glass substrates were positioned vertically on a specially designed substrate holder and rotated in the reactive solution with a speed of 50 ± 2 rpm. The temperature of the solution was then allowed to rise slowly to 308 K. The substrates were subsequently removed from the beaker after 2 h of deposition. The films thus deposited were washed by distilled water, dried in air and preserved in the desiccator.

2.4. Characterization of $CuInSe_2$ thin films

The X-ray diffraction study of CIS thin film was carried out using Cr$K\alpha_1$ radiation on Philips PW-1710 diffractometer ($\lambda = 2.28970$ Å). The thickness of the film was calculated by the weight difference method. The electrical conductivity of CIS thin film was measured using a 'dc' two-probe method. An ohmic contact was provided by

* Corresponding author. Tel.: +91 231 2609381; fax: +91 231 2605271.
E-mail address: p_hankarep@rediffmail.com (P.P. Hankare).

0925-8388/$ – see front matter © 2010 Published by Elsevier B.V.
doi:10.1016/j.jallcom.2010.03.215

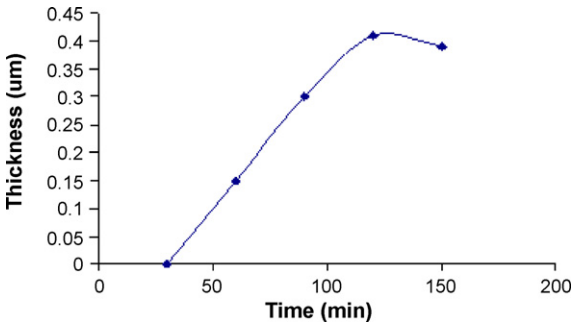

Fig. 1. Variation of the film thickness with deposition time (min).

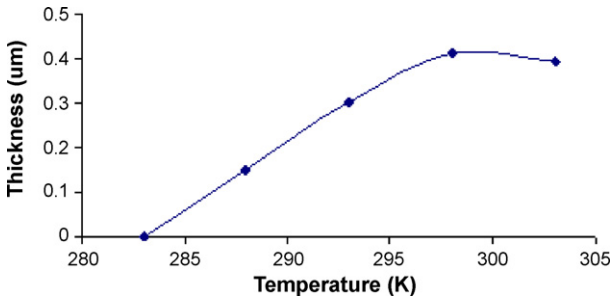

Fig. 2. Variation of the film thickness with deposition temperature (K).

applying air drying silver paste at the ends of the film. The measurement of conductivity was carried out using a constant voltage of 30 V across the sample and noting the current at different temperatures. Thermoelectric power was measured by maintaining a temperature gradient along the length of a film. The potential difference between the two points of contact separated by 1 cm was recorded with a digital microvoltmeter. A calibrated thermocouple (chromel–alumel, 24 gauges) was used to sense the working temperature. The optical absorption measurement was made in the wavelength range of 400–800 nm using a Hitachi-330 (Japan) UV–VIS–NIR double beam spectrophotometer at room temperature. An identical, uncoated non-conducting glass substrate was used as a reference for the absorption correction. The analysis of the spectrum was carried out by computing the values of absorption at every step of 5 nm. A 250MK-III Stereoscan (USA) scanning electron microscope (SEM) was used for the surface morphological study. The film composition analysis was determined using Perkin-Elmer-3030 atomic absorption spectrophotometer.

3. Results and discussions

3.1. Growth mechanism

In the reaction bath, Cu^{+1} and In^{+3} were complexed with tartaric acid in the form of water soluble tartarate complex which controls the metal ion concentration. The dissociation of sodium selenosulphate as well as tartarate complex in alkaline medium takes place at room temperature. It forms a clear solution and no film or precipitate is observed even after a long time, indicating formation of a stable complex state metal ions. The process is controlled by the slow release of Cu^{+1}, In^{+3} and Se^{-2} ions in the solution. However, due to the reducing action of hydrazine hydrate, Cu^{+1} ion is deposited and the ion by ion deposition takes place on the glass substrate to form uniform, stoichiometric $CuInSe_2$ film. The growth kinetics of the film can be understood from the following reactions:

$$Cu^{+1} + 2TA^{2-} \rightarrow [Cu(TA)_2]^{3-} \quad (1)$$

$$In^{+3} + 3TA^{3-} \rightarrow [In(TA)_3]^{3-} \quad (2)$$

$$Na_2SeSO_3 + OH^- \rightarrow Na_2SO_4 + HSe^- \quad (3)$$

$$HSe^- + OH^- \rightarrow H_2O + Se^{-2} \quad (4)$$

$$[Cu(TA)_2]^{3-} + [In(TA)_3]^{3-} + 2Se^{-2} \rightarrow CuInSe_2 + 5TA^{2-} \quad (5)$$

Hydrazine hydrate also acts as a complementary complexant, which improves the compactness and adherence of the film. It has been observed that at higher rotation speeds (>50 rpm) thinner films deposit while at the lower speed (<45 rpm) thicker non-adherent films are formed. We could obtain uniform, brown red colored well adherent film at optimum rotation (~50 rpm). Thickness of the film measured as a function of time in minutes is shown in Fig. 1. The optimum thickness was also measured as a function of temperature and the variation there of is shown in Fig. 2. The thickness is found to increase linearly with temperature up to 300 K and then onward decreases sharply. This might be due to faster release of Cu^{+1}, In^{+3} and Se^{-2} ions forming their precipitates instead of formation of film. The terminal film thickness was found to be 0.41 μm.

3.2. Structural study

The semiconducting CIS exists in the tetragonal phase structure. The structural investigation of CIS thin film annealed at 573 K was carried out using $CrK\alpha_1$ radiation in the 2θ range of 20–100°. The XRD pattern is shown in Fig. 3. The observed and standard 'd' values (ASTM card no. 23-0209) are listed in Table 1. The CIS thin film shows prominent peaks of (1 1 2), (2 2 0), and (3 1 2) planes. The observed lattice parameter is in fairly good agreement with standard value ($\alpha = \beta \neq \gamma$, 5.69 = 5.64 ≠ 11.57) [15]. The average crystallite size of the material was determined by using the Scherrer formula:

$$D = \frac{K\lambda}{\beta \cos\theta} \quad (6)$$

where D is the crystallite size (in Å), λ is the X-ray wavelength used (in Å), β is the full width at half maximum (in radians), θ is the Braggs diffraction angle and K is constant (0.9).The crystallite size was calculated by resolving the highest intensity peak. The average crystallite size of the annealed CIS thin film was found to be 331 Å.

3.3. Morphological studies

Scanning electron microscopy is used to study the surface morphology of the sample. The SEM micrographs as annealed $CuInSe_2$ thin films at 5000× magnification are shown in Fig. 4. The $CuInSe_2$ micrograph shows a compact structure composed of a single type of small, densely packed microcrystals. The grains are well defined, spherical and of almost similar size. The annealed sample shows improvement in grain size. The increase in grain size leads to increase in the grain boundaries. The presence of fine background is an indication of one step growth by multiple nucleations. The grain

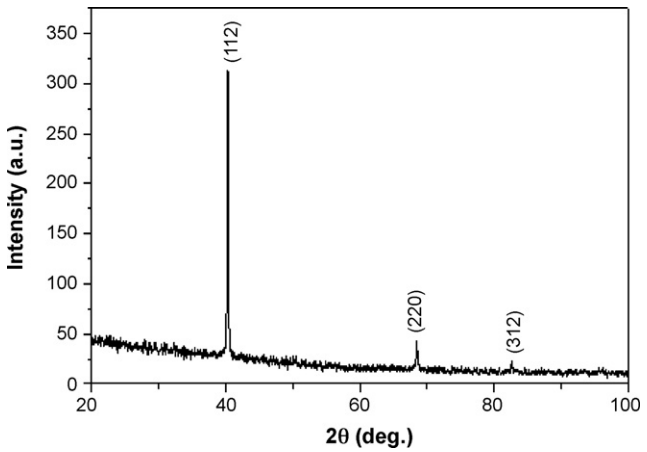

Fig. 3. XRD pattern of $CuInSe_2$ thin film.

Table 1
Crystallographic optical and electrical parameter of $CuInSe_2$ thin films.

Film	*d*-Value (Å)		Plane (*h k l*)	Band-gap (eV)	Activation energy (eV)	Specific resistivity $(\Omega\,cm)^{-1}$	
	Observed	Standard (ASTM)			H.T.	300 K	500 k
$CuInSe_2$	3.330 2.036 1.737	3.340 2.040 1.743	112 220 312	1.1	0.2446	10^2	10^1

size calculated from SEM is matchable with grain size calculated by XRD.

3.4. Compositional analysis

Atomic absorption spectroscopy (AAS) was used to study compositional analysis by calibration curve method. The weighed quantity of sample was dissolved in the minimum quantity of concentrated HNO_3 [16]. Below pH = 7, the selenium was precipitated as free element while nitrates of copper and indium remain in the solution. The precipitate was filtered through a Gooch crucible and subjected to selenium estimation using a standard gravimetric method. The filtrate containing copper nitrate and indium nitrate was diluted to suitable dilution and estimated by AAS. The standard solution used for obtaining the calibration curve was made by diluting commercial standards to concentration 0.4, 0.8, 1.2, 1.6, 2.0 mg/mL for copper and indium. The compositional analysis of the sample using AAS gave percentage of copper 24.62%, indium 21.06% and selenium 54.32% indicating indium deficiency. The Cu/In ratio is found to be 1.16, while the analysis techniques indicate the presence of higher selenium.

3.5. Optical and electrical studies

The optical absorption measurement was recorded in the range of 400–800 nm at room temperature neglecting losses due to scattering and transmission. The data were systematically studied in the vicinity of the absorption edge on the basis of three-dimensional model. The simplest form of equation obeyed near and above absorption edge is [17]:

$$\alpha h\nu = A(h\nu - E_g)^n \quad (7)$$

where, α is absorption coefficient, $h\upsilon$ is the photon energy (eV), A and n are the constants. A is complex parameter, which depends on temperature and photon energy, E_g is the direct band-gap energy. A plot of $(\alpha h\upsilon)^2$ versus $h\upsilon$ is expected to be a straight line whose intercept to the X-axis gives the optical band-gap. The graph of $(\alpha h\upsilon)^2$ versus $h\upsilon$ for as-deposited film is shown in Fig. 5. The band-gap of $CuInSe_2$ was found to be 1.1 eV, which is comparable to the band-gap of $CuInSe_2$ thin film observed by other investigators [4].

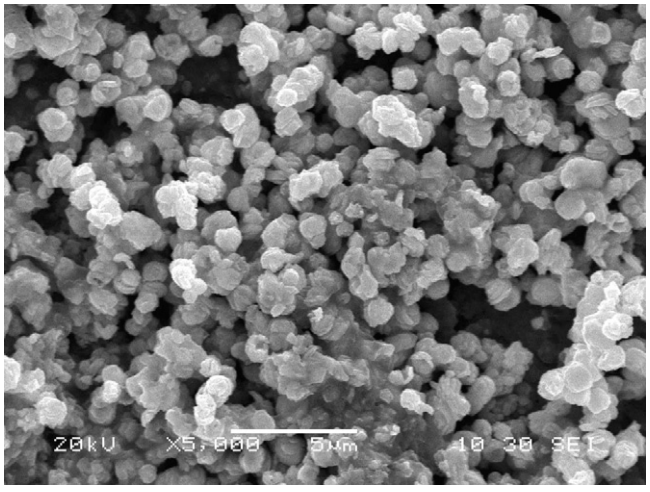

Fig. 4. SEM images of $CuInSe_2$ thin film.

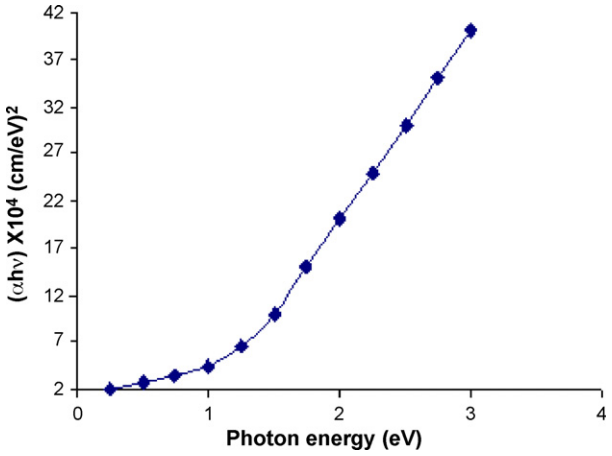

Fig. 5. Plots of $(\alpha h\nu)^2$ versus photon energy.

3.6. Electrical properties

The electrical resistivity of the sample was measured in the temperature range of 300–500 K. Fig. 6 shows the variation of logarithm of resistivity for the as-deposited CIS film. The resistivity decreases with increase in temperature indicating the semiconducting behavior of $CuInSe_2$ thin films. Electrical resistivity at room temperature was found to be of the order of 10^2 $(\Omega\,cm)$. It has been reported that the value of electrical resistivity varies from 10^1 to 10^3 $(\Omega\,cm)$ for the sample with copper excess to indium excess films, respectively [6]. The activation energy is calculated using the Arrhenius equation:

$$\rho = \rho_0 \exp\left(-\frac{Ea}{kT}\right) \quad (8)$$

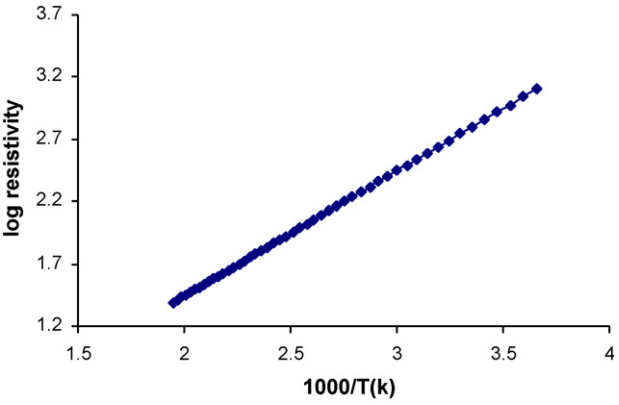

Fig. 6. Arrhenius plot showing variation of conductivity with temperature.

where, ρ is the resistivity, ρ_0 is a constant, *Ea* is the thermal activation energy, k is the Boltzmann constant and T is the absolute temperature. The activation energy obtained from the high temperature regions is found to be 0.244 eV, respectively.

The thermoelectric power measurement was used to determine the type semiconductors. For the thermoelectric power measurements, the open circuit thermo-voltage generated by the sample, when a temperature gradient is applied across a length of the sample was measured using a digital microvoltmeter. The temperature difference between the two ends of the sample causes transport of carriers from the hot to cold end, thus creating an electric field, which gives rise to thermo-voltage across the ends. The thermo-voltage generated is directly proportional to the temperature gradient maintained across the semiconductor ends. From the sign of the potentiometer terminal connected at the cold end, one can deduce the sign of predominant charge carriers. In the case of $CuInSe_2$ thin films studied by us the negative terminal was found to be at the cold end; therefore, the film shows n-type conduction mechanism [4,18].

4. Conclusions

A uniform, well adherent thin film of ternary $CuInSe_2$ has been deposited using a simple chemical bath deposition technique at room temperature. X-ray diffraction studies show formation of tetragonal $CuInSe_2$ structure. The film is highly absorptive and shows direct type of transition. The band-gap is found to be of the order of 1.1 eV. The specific resistivity at room temperature of $CuInSe_2$ thin film is found to be of the order of 10^2 (Ω cm). Thermoelectric power measurement shows n-type conduction for $CuInSe_2$ thin film.

References

[1] L. Jianzhuang, Z. Xiujian, X. Donglin, J. Wuhan Univ. Technol.: Mater. Sci. Ed. 22 (1) (2007) 140.
[2] J.R. Tuttle, E.D. Cole, K.R. Ramanathan, M. Contreras, J. Alleman, J. Kcane, Noufi, Proceeding of the 10th Sunshine Workshop Thin Film Solar Cells, Tokyo, Japan, November 8–9, 1996, p. 139.
[3] L. Stolt, Proceedings of 9th International Phovoltaic Science and Engineering Conference, Niyazaki, Japan, November 11–15, 1996, p. 139.
[4] A. Ashour, A.A. Ramdhan, K. Abd El-Hady, A.A. Akl, J. Mater. Sci.: Mater. Electron. 16 (2005) 599.
[5] M.B. Dergacheva, V.V. Chaikin, Russ. J. Appl. Chem. 81 (2008) 614.
[6] N. Kavear, M. Hyland, R. Hill, Turk. J. Phys. 17 (1993) 818.
[7] V.Yu. Rud, Yu.V. Rud, Semiconductors 33 (1999) 870.
[8] F.R. White, A.H. Clark, M.C. Gxaf, J. Appl. Phys. 50 (1979) 544.
[9] A. Gary, Mitchell, J. Sol. Energy Mater. Sol. Cells 57 (1996) 57.
[10] J.M. Merino, M. Leon, F. Rueda, J. Thin Solid Films 22 (2000) 361.
[11] H.K. Song, S.G. Kim, H.J. Klm, J. Sol. Energy Mater. Sol. Cells 75 (2003) 145.
[12] R.N. Bhattacharya, W. Batchelor, J.E. Granata, J. Sol. Energy Mater. Sol. Cells 55 (1998) 83.
[13] M. Pattabi, P.J. Sebastain, X. Mathew, J. Sol. Energy Mater. Sol. Cells 63 (2000) 315.
[14] P.P. Hankare, A.S. Khomane, P.A. Chate, K.C. Rathod, K.M. Garadkar, J. Alloys Compd. 469 (2009) 478.
[15] ASTM, Data file no. 23-0209.
[16] P.P. Hankare, P.A. Chate, M.R. Asabe, S.D. Delekar, I.S. Mulla, K.M. Garadkar, J. Mater. Sci.: Mater. Electron. (2006).
[17] J. Bardeen, F.J. Blutt, L.H. Hall, in: R. Brechepride, B. Russel, E. Hahn (Eds.), Proceedings of the Photo-Conductivity Conference, Wiley, NY, 1975.
[18] W. Siefert, Thin Solid Films 120 (1984) 267.